High-Frequency Operation of a DC/AC/DC System for HVDC Applications

Thomas Lüth, *Student Member, IEEE*, Michaël M. C. Merlin, *Member, IEEE*, Tim. C. Green, *Senior Member, IEEE*, Fainan Hassan, *Senior Member, IEEE*, and Carl D. Barker, *Senior Member, IEEE*

***Abstract*—Voltage ratings for HVdc point-to-point connections are not standardized and tend to depend on the latest available cable technology. DC/DC conversion at HV is required for interconnection of such HVdc schemes as well as to interface dc wind farms. Modular multilevel voltage source converters (VSCs), such as the modular multilevel converter (MMC) or the alternate arm converter (AAC), have been shown to incur significantly lower switching losses than previous two- or three-level VSCs. This paper presents a dc/ac/dc system using a transformer coupling two modular multilevel VSCs. In such a system, the capacitors occupy a large fraction of the volume of the cells but a significant reduction in volume can be achieved by raising the ac frequency. Using high frequency can also bring benefits to other passive components such as the transformer but also results in higher switching losses due to the higher number of waveform steps per second. This leads to a tradeoff between volume and losses which has been explored in this study and verified by simulation results with a transistor level model of 30-MW case study. The outcome of the study shows that a frequency of 350 Hz provides a significant improvement in volume but also a penalty in losses compared to 50 Hz.**

***Index Terms*—DC–DC power conversion, HVdc converters, HVdc transmission, multilevel converters.**

I. Introduction

A NUMBER of high-voltage dc (HVdc) schemes are currently under development and consideration in Europe. The interest in HVdc is driven by the expansion of renewable generation capacity in places such as Scotland, Germany, and the North Sea [1], as a means to efficiently transmit the generated power to far away load centres. As most of the currently considered (or already built) schemes are of the point-to-point type which, coupled with the absence of a common dc grid code, allows the voltage ratings to be freely chosen by each developer. As a result the voltage rating is often a function of the available cable technology at the time of development.

One of the most likely pathways for an HVdc grid to develop is from the interconnection of point-to-point schemes, at some point in the future [2]. This will require dc/dc voltage conversion technology for HVdc applications.

The voltage conversion ratio has important implications on the converter technology as it influences the magnitude of currents and amount of stress imposed on the system. The same nomenclature as defined in [3] has been adopted for this paper. As such, a low step ratio is defined as per (1)

$$V_{\text{dc high voltage side}}/V_{\text{dc low voltage side}} \leq 1.5. \quad (1)$$

A low step ratio could be used to interconnect existing HVdc networks of different nominal voltages. Connections to a dc collection grid of an off-shore wind farm, a number of which are planned in the North Sea, may require a medium step ratio which is defined in (2)

$$1.5 < V_{\text{dc high voltage side}}/V_{\text{dc low voltage side}} \leq 5. \quad (2)$$

This paper presents a possible dc/dc system for low to medium step-ratio applications. It consists of two ac/dc converters coupled through a transformer in what might be described as "front-to-front" connection. The transformer provides galvanic separation between the two dc connections as well as the voltage step. Such a system could be used to interconnect existing HVdc schemes in the process of building up a larger HVdc network. It may also be used to tap-into an existing HVdc link to connect an off-shore wind park for example. Furthermore, if interconnection between two HVdc networks is desired with separate grounding arrangements, then the galvanic separation provided by the transformer of this system may allow for this.

Voltage source converters (VSCs) are generally considered to be the best option of for multiterminal HVdc grids [2] as they allow power reversal without having to change the voltage polarity and can connect to weak ac networks. Consequently, two well-studied multilevel VSC topologies are considered for use in the dc/ac/dc system. These converters are the modular multi-level converter (MMC) [4] and the alternate arm converter (AAC) [5], [6]. Both make use of either half-bridge or full-bridge cells in their valves to generate a staircase voltage waveform with small voltage steps. This allows individual switching devices in the cells to be at a lower frequency compared to older VSC topologies such as the two-level or three-level converters [7]–[9]. Due to this, modular multilevel topologies achieve a significant reduction in switching losses. The AAC differs from the MMC in its mode of operation in that its arms conduct alternatively for only half a cycle, allowing fewer cells to be used but at the expense of additional director switches consisting of series-connected IGBTs.

Manuscript received July 1, 2013; revised September 12, 2013; accepted November 7, 2013. Date of current version March 26, 2014. This work was supported by Alstom Grid and the Engineering and Physical Sciences Research Council under Grant EP/G066477/1. Recommended for publication by Associate Editor J. H. R. Enslin.

T. Lüth, M. M. C. Merlin, and T. C. Green, are with the Imperial College London, London SW7 2AZ, U.K. (e-mail: tl306@ic.ac.uk; mmm107@ic.ac.uk; tcg@ic.ac.uk).

F. Hassan and C. D. Barker are with the Alstom Grid, Stafford ST17 4LX, U.K. (e-mail: fainan.hassan@alstom.com; carl.barker@alstom.com).

Color versions of one or more of the figures in this paper are available online at http://ieeexplore.ieee.org.

Digital Object Identifier 10.1109/TPEL.2013.2292614

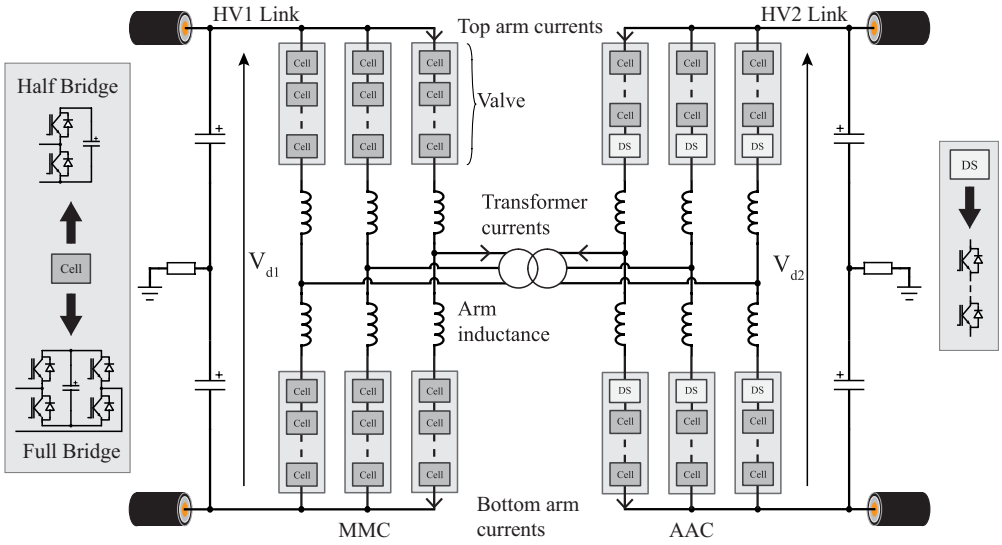

Fig. 1. Circuit diagram of a VSC-based transformer coupled dc/ac/dc system. Both VSC topologies considered are shown in the figure: to the left the MMC and to the right the AAC. "DS" in the AAC valve refers to the director switch which replaces some of the cells.

Alternative dc/dc topologies utilizing the multilevel cell blocks are beginning to be considered [10] along with other circuit concepts, such as presented in [11]. These circuits however do not offer the galvanic isolation offered by a transformer which can be useful in some abnormal operating conditions and for separating grounding arrangements for different parts of a dc network. Furthermore, the well-established switch-mode dc/dc converters, typically employed for low-power applications, do not tend to scale very well for high-power applications [12], [13].

II. Operational Concept of DC/AC/DC System

The suggested front-to-front arrangement of two ac/dc converters is shown in Fig. 1. For the sake of argument both converter types are shown in this diagram. The system topologies investigated use either two MMCs or AACs. Each is connected to one dc link, which are assumed to be of different dc voltages, and are connected together on their ac side through a coupling transformer.

A three-phase arrangement as shown in Fig. 1 is analyzed in this paper but the number of phases ultimately is a design choice. The number of phases of such a system however remains a tradeoff between the volume required for additional phase-legs and dc side filters and the losses incurred. In a three-phase arrangement, the ac currents generated by each phase, combine to form a dc side current with only a small sixth harmonic ripple.

Fig. 1 depicts both VSCs considered in this paper. The main difference in the circuit topology between the two is in the valves (where a valve refers to a combination of cells connected between an ac phase connection and a dc terminal). The MMC's valves consist entirely of cells. In the AAC some of the cells are replaced with Director Switches (DS). In both converters, the cells can be either of the full-bridge or half-bridge variety.

In the MMC, half of the ac current flows through each arm during the full cycle in addition to a dc current. The AAC differs in its operation compared to the MMC by conducting the full ac current through the top or bottom arms alternatively for half of the ac cycle [6]. When the other arm is not conducting any current, its director switch opens breaking the current path and blocking the remaining voltage difference between the ac voltage and the cell stack. The valve in the conducting arm is thus responsible for generating the ac waveform.

A. Energy Balance in the Valves

In the MMC, the energy exchanged between a valve and the ac link is characterized by the ac voltage and current as per (3) (Φ_I is the angle of the ac current with respect to the ac voltage). Energy balance has also been discussed in [14]

$$\mathrm{E}_{\mathrm{AC\ MMC}} = \frac{\pi \hat{V}_{\mathrm{ac}} \hat{I}_{\mathrm{ac}}}{2\omega_0} \cos\left(\Phi_I\right). \tag{3}$$

Each stack conducts half of the ac current for the full duration of every cycle. Therefore, there will be no net energy exchange between the valve and the dc link due to the ac current. To achieve an energy exchange a dc current has to be run through the phase leg $I_{d\ \mathrm{phase}}$ as described next

$$\mathrm{E}_{\mathrm{DC\ MMC}} = \frac{\pi V_d I_{d\ \mathrm{phase}}}{\omega_0}. \tag{4}$$

To maintain zero net energy drift in the valve, the ac and dc energy exchanges in the MMC need to be matched. For any given ac power demand an appropriate dc arm current will therefore be applied.

Each valve in the AAC only conducts the ac current for half of each cycle which affects the energy management of the valves. The energy exchange with the ac side is the same as for the MMC as shown as follows:

$$\mathrm{E}_{\mathrm{AC\ AAC}} = \frac{\pi \hat{V}_{\mathrm{ac}} \hat{I}_{\mathrm{ac}}}{2\omega_0} \cos\left(\delta_{\mathrm{ac}}\right). \tag{5}$$

The energy exchanged between each valve and the dc side is shown as

$$\mathrm{E}_{\mathrm{DC\ AAC}} = \frac{V_d \hat{I}_{\mathrm{ac}}}{\omega_0} \cos\left(\delta_{\mathrm{ac}}\right). \tag{6}$$

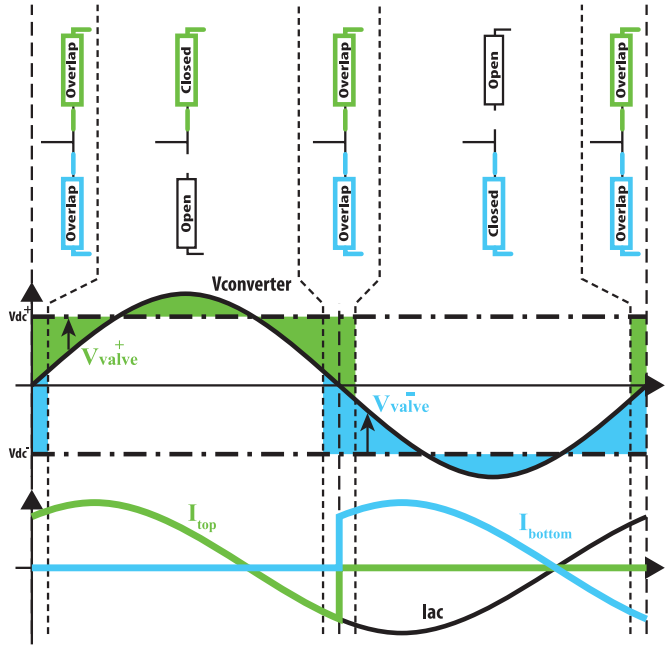

Fig. 2. Definition of the overlap period in an AAC.

These two energy flows are matched (neglecting losses) only at one particular ac voltage magnitude for any given dc-link voltage. This ac voltage is commonly referred to as the "sweet-spot" voltage and is described in (7) and [6]. Operating at the sweet-spot implies zero net energy drift in the valves

$$\hat{V}_{\text{AC sweet-spot}} = \frac{2V_d}{\pi}. \tag{7}$$

Some balancing action will still be required however: operation at the exact sweet-spot is not practical not least because of the voltage waveform distortion due to the discrete voltage steps of the valve levels. Also, vertical balancing action may be required during the operation to maintain equal energy balance in both valves of the same phase leg. This is also true for the MMC for which balancing methods as described in [14] can be used.

To enable energy balancing in the AAC, an overlap period (Φ_{ol}) is introduced as discussed in [6]. This is a period centered around the zero crossing of the ac voltage. This marks the instance when one arm hands over the conduction of the ac current to the other. During the overlap period both director switches in a phase leg are closed as illustrated in Fig. 2. This completes a conduction path for a dc current to be run through both valves and the dc link. By this mechanism energy can be exchanged between the dc link and the valves. By modulating the overlap current waveform energy can be exchanged between the top and bottom valves.

Even when the energy flows from the dc and ac side are matched on average over one cycle in either converter topology, it is important to note that the valves will still experience an energy deviation during the cycle. This is because the ac and dc side energy flows are not matched at every instant during a cycle. This energy deviation is referred to as the intracycle energy deviation. This is of particular importance to find the theoretical minimum capacitance required for the converters as further discussed in Section C.

B. AC-Link Parameters

As the ac link is fully internal to this system, its parameters are not limited by any grid-codes and can be adjusted to achieve better efficiency or minimize the physical size of the system for example. The ac voltages magnitudes at which both converters operate at can be freely chosen. Similarly the ac frequency is not limited to 50 or 60 Hz.

To minimize the power losses it is advantageous to keep the ac current magnitude as low as feasible in a converter, usually by increasing the voltage level of the system. In the case of the MMC this means it is typically operated with a peak ac phase voltage equal to half of the dc-link voltage $(V_d/2)$. This is the highest ac voltage which can be generated by using only half-bridge cells.

A peak ac voltage larger than the dc terminal voltage, i.e., $V_d/2$, requires the valves to "add" to the dc-link voltage during some parts of the ac waveform. This in turn requires full-bridge cells which have twice as many switching devices in the conduction path as half-bridge cells. A valve that is generating a voltage to increase the ac voltage above the dc terminal voltage is commonly referred to as operating in "over-modulation" mode. A valve that is generating a voltage to only "subtract" from the dc-link voltage, is said to be "under-modulating."

The AAC is typically operated at its sweet-spot voltages to minimize the need for additional energy balancing of the cells. From (7), it can be seen that sweet-spot operation requires a peak ac voltage that is 27% larger than half of the dc-link voltage. The converter is therefore required to overmodulate.

Each phase is assumed to be connected via a single-phase transformer. The initial assumption, used in this paper, is that each transformer is connected to the midpoint of the capacitors of either converter which in turn is grounded. Other three phase arrangements can be considered. Furthermore, third-harmonic injection techniques, as presented in [15], [16] can be applied here. The ac waveforms are sinusoidal so no special transformer design has been considered for this investigation.

Raising the ac frequency above a typical network value of 50 Hz for example, can be advantageous for the passive component sizing. Assuming all else remains constant, the core volume of an ideal transformer is inversely proportional to the ac frequency. While we recognize that in practice this may not be realized because of other limitations on the transformer's core design such as heat extraction equipment and winding insulation, the total volume of the core is expected to decrease significantly with increasing frequency.

Furthermore, an increase in ac frequency will reduce the peak intracycle energy deviation of each cell. This can in turn significantly reduce the minimum cell capacitor size required, as explained in further detail in the next section. The cell capacitor remains the largest component of cell as illustrated in Fig. 3. Reducing the capacitance of the cell will allow for further volume savings.

C. Minimum Cell Capacitance

Each cell capacitor is typically designed to operate within a voltage band in order to keep the converter stable and prevent the capacitors to overcharge. Due to the intracycle energy

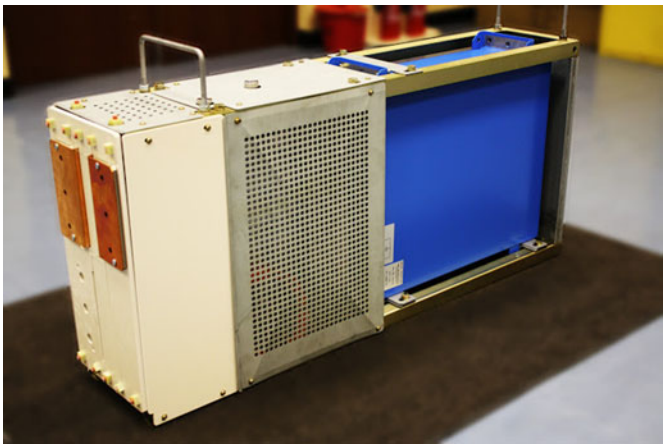

Fig. 3. Single cell as built by Alstom Grid. The blue component in the back is the cell capacitor (image from www.alstom.com/uk).

fluctuations experienced by the valves, it is important to size the capacitors such that the largest intracycle energy deviation does not result in a cell voltage deviating outside the allowed range.

The peak intracycle energy deviation can be found by considering all the current flowing through the valve and the voltage it generates during a cycle. The minimum cell capacitance $(\check{C}_c)$ can be calculated from the peak absolute energy deviation $(|\Delta\hat{E}|)$ experienced by a valve and the number of cells in it (n_C) as described next

$$\check{C}_c = \frac{2|\Delta\hat{E}|}{n_C \Delta V^2}. \tag{8}$$

The variable ΔV^2 describes the maximum voltage deviation squared. This value is calculated differently depending on if the energy deviation is causing the cells to absorb or release energy. This will determine if the upper or lower limits of the allowed cell voltage are used ($\hat{V}_c$ and $\check{V}_c$ respectively) as per (9). In this paper, the nominal operating voltage of a cell has arbitrarily been chosen as 1.8 kV with lower and upper limits of 1.5 kV and 2.1 kV, respectively

$$\Delta V^2 = \begin{cases} \hat{V}_c^2 - V_c^2 & \text{if } \Delta\hat{E} < 0 \\ V_c^2 - \check{V}_c^2 & \text{if } \Delta\hat{E} \geq 0 \end{cases}. \tag{9}$$

The peak intracycle energy deviation is found numerically by calculating the valve energy, as described by (10), in small time-steps (t_{step}) over one ac cycle. $V_{\text{st}}(t)$ denotes the voltage across the stack as described in (11). $I_{\text{st}}(t)$ is the current flowing through the stack which is described differently for the MMC and AAC and takes the ac components as well as the dc balancing current into account. Also, the peak intracycle energy deviation is a function of frequency since the energy flow equations given in (3) to (6) are too. With increasing ac frequency the energy deviation will decrease

$$E^k_{\text{valve}} = E^{k-1}_{\text{valve}} + t_{\text{step}} \cdot V_{\text{st}}(k \cdot t_{\text{step}})\, I_{\text{st}}(k \cdot t_{\text{step}}) \tag{10}$$

$$V_{\text{st}}(t) = \frac{V_d}{2} - \hat{V}_{\text{ac}} \sin(\omega_0 t). \tag{11}$$

The minimum cell capacitance calculated in this way is a good indicator to compare different operating points and converter topologies against each other. It should be noted that this capacitor sizing methodology assumes that the effect of the energy deviation during a cycle is split evenly between all cells in a valve. The cells are typically rotated in their duty during a cycle to prevent any one cell voltage from drifting too far away from other cell voltages. The cell's voltages are sorted and utilized to take advantage of the direction of the arm current similar to the method described in [15]. A cell rotation event includes the resorting of the cell voltages and occurs at constant intervals over a cycle.

In between rotations voltage drifts may occur in individual cells. The minimum capacitor value calculated this way assumes instantaneous energy duty balancing among all the cells in a valve at every instant to ensure an evenly split voltage deviation among all the cells. This makes this capacitance value a theoretical lower limit which in practice will be higher as this cannot be achieved with a finite cell rotation frequency. Typically, a margin would be added to the minimum to account for this.

High cell rotation frequencies incur significant switching loss penalties. Therefore, a compromise between cell rotation frequency and capacitor volume has to be made. In this paper, a rotational frequency of 16 rotations per ac cycle has been assumed for all ac frequencies investigated. The effect of this on the switching losses can be seen from the loss results for the case-study system in Section IV.

D. Number of Devices in the Valves

The number of cells in the valves of a multilevel converter depends on the maximum voltage that these stacks have to generate. In the MMC, each valve has to be able to generate the voltage between the dc terminal voltage and the negative peak ac voltage. Assuming each cell is charged at a voltage of magnitude V_C, the number of cells per arm is calculated as per (12) to support the peak voltage across each arm [4]

$$n_{C\,\text{MMC}} = \frac{V_d/2 + \hat{V}_{\text{ac}}}{V_C}. \tag{12}$$

A valve in the AAC will have to provide both overmodulation and under-modulation voltages. They can be found through (13) and (14), respectively [6], [12]. The larger of the two voltages will dictate the minimum number of cells in each valve. In the case of operation at the sweet-spot voltage this is the under-modulation voltage requirement

$$\hat{V}_{\text{valve}\,UM} = \frac{V_d}{2} + \hat{V}_{\text{ac}} \cdot \sin\left(\frac{\Phi_{\text{ol}}}{2}\right) \tag{13}$$

$$\hat{V}_{\text{valve}\,OM} = \hat{V}_{\text{ac}} - \frac{V_d}{2}. \tag{14}$$

The number of devices in the conduction path (n_{DiCP}) per arm can be considered to compare different operating parameters and converter topologies against each other. n_{DiCP} is the number of switching devices in the conduction path in each arm at any point in time. Both the devices from the cells as well as

TABLE I
GENERAL CASE STUDY SYSTEM PARAMETERS

- ±30 MW power transfer capability
- HV1 DC link voltage: ±25 kV
- HV2 DC link voltage: ±15 kV
- DC/DC step ratio: 1.7

TABLE II
MMC FRONT-TO-FRONT SYSTEM PARAMETERS

Parameter	HV1 MMC	HV2 MMC
Peak AC voltage	25 kV	15 kV
Cells per arm	28	17
Cell type	Half-bridge	Half-bridge
n_{DiCP} per phase leg	56	34

TABLE III
AAC FRONT-TO-FRONT SYSTEM PARAMETERS

Parameter	HV1 AAC	HV2 AAC
Peak AC voltage	31.8 kV	19.1 kV
Cells per arm	17	10
Cell type	Full-bridge	Full-bridge
DS per arm	15	9
n_{DiCP}[a] per phase leg	49	28

[a] DS: Director Switches. Each director switch device is considered to be rated at the nominal cell voltage of 1.8 kV.

from the director switches (as far as applicable) are considered for this. Therefore, the number heavily depends on the type of cell used in the valve: a half-bridge cell will add one whereas a full-bridge two switching devices into the conduction path. The number of devices in the conduction path along with the current magnitudes affecting these devices provides an indication of the relativelosses of one converter compared to another. As such it should be noted that the MMC's arm currents flow for the full duration of the cycle whereas the AAC's do not. A more comprehensive comparison of the different converters is presented later in this paper with the aid of a case-study system.

E. Case Study System

A simulation model was developed in Simulink to verify the operability of the system. Although this converter topology is suitable for HVDC applications, typically rated for hundreds of kilovolts and hundreds of megawatts, the simulation model was scaled for significantly lower voltage and power levels. Indeed, the system has been modeled down to the transistor level and realistic voltage ratings would require a large number of switches to be modeled which would make the simulation too computationally complex to be practical. The system was modeled in such a detail to accurately estimate the losses using model specific postprocessing scripts and to verify the cell level operation. Parameters common to all simulations of the case study system are listed in Table I.

Two different system topologies were modeled: one with two MMCs and one with two AACs. The converter parameters are listed in Tables II and III. The cell capacitance for the 50 Hz simulation was set to 7 mF for both converters. As the number of cell rotations per cycle was kept constant for both ac frequencies, the cell capacitance could be reduced to 1 mF for the 350 Hz simulations.

TABLE IV
TRANSFORMER PARAMETERS IN MMC SYSTEM

Parameter	At 50 Hz	At 350 Hz
Coupling factor	0.995	0.995
Magnetising L	5.9 H	0.8 H
Primary leakage L	29.8 mH	4.3 mH
Secondary leakage L	10.8 mH	1.6 mH

From the converter parameters, the distinct difference between the AAC and MMC can be noted: The MMC's cell stacks have to be able to support the entire ac waveform and therefore require significantly more cells than the AAC's. It is not required to generate an ac voltage above that of the dc terminal but only requires half-bridge cells. Its n_{DiCP} is however not lower than the AAC's because its arms are continuously conducting the ac and dc currents. whereas the in the AAC each arm is only conducting the ac voltage for one half-cycle.

The overlap period of the AAC was kept constant at 18° for all simulations. This translates into a time period of 1 ms per half-cycle at an ac frequency of 50 Hz and into 0.14 ms per half-cycle at 350 Hz ac.

The arm inductance in the AAC is primarily required to control the overlap currents. Thus, scaling it down with frequency incurs very little extra switching losses and makes the ramping of the overlap-currents easier. Scaling down the arm inductance with ac frequency in the MMC in a similar fashion results in noticeably higher switching losses as the dc current flowing through the arms has to be controlled for the full duration of the cycle. The arm inductance values at 50 Hz were arbitrarily chosen to maintain current control in the converters without additional switching by the cells. The MMC's valves are continuously in conduction and can therefore be thought of as three series-connected pairs of voltage sources in parallel with a series-connected pair of voltage sources modelling the dc terminals. Small differences in voltage of each of the valve's voltages sources can lead to large dc currents flowing between them. The arm inductances serve to counteract this and limit the rate of change of the arm currents. Due to the discontinues, conduction in the arms smaller arm inductances can be used in the AAC as both valves in the same phase are only in conduction simultaneously for a short overlap period during each cycle. In the AAC, the arm inductance value is a tradeoff between the volume and conduction losses due to it and the additional switching losses incurred during the overlap period to maintain current control. The arm inductance for the MMC was kept at 1 mH for all frequencies. In the AACs, an arm inductance of 0.7 mH was used at 50 Hz and 0.1 mH at 350 Hz.

The single-phase transformer was modeled using a mutual inductance model. No resistive elements were included in the time domain simulation model of the transformer. The transformer parameters for 50 and 350 Hz are listed in Tables IV and V. The transformer models vary slightly as the magnetizing inductance was sized based upon a fixed fraction of the secondary current's magnitude of 1%.

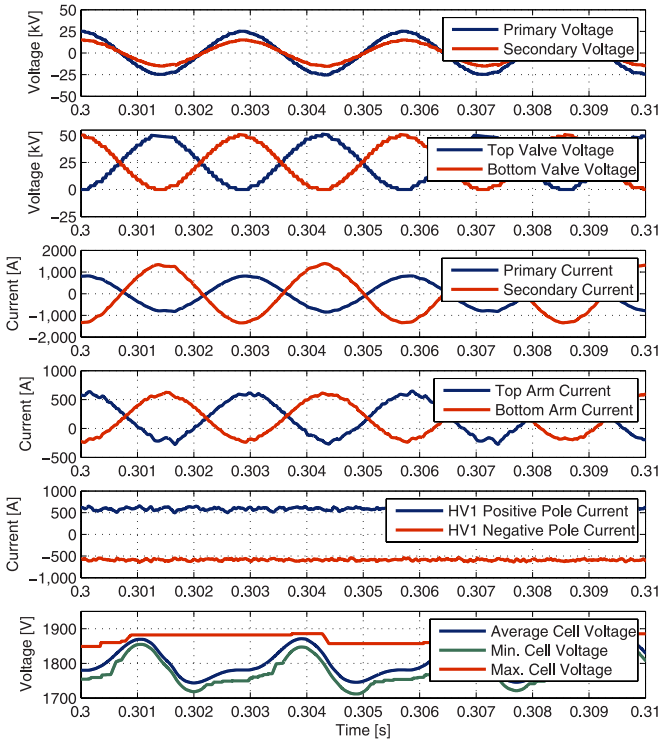

Fig. 4. MMC front-to-front system topology voltages and currents for case study system and 350-Hz ac link. Valve voltages and arm currents are shown for a single phase leg of the HV1 MMC. The cell voltages are shown for the top valve in same phase of the HV1 MMC.

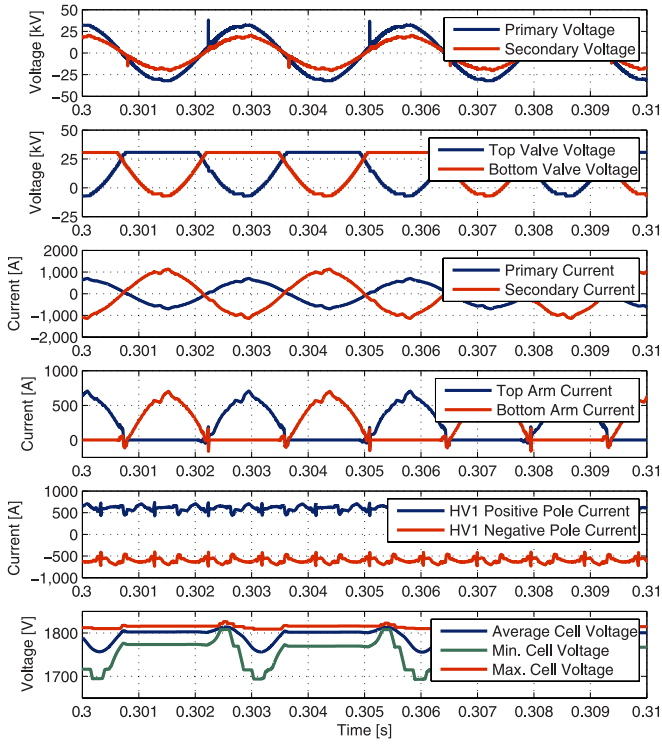

Fig. 5. AAC front-to-front system topology voltages and currents for case study system and 350-Hz ac link. Valve voltages and arm currents are shown for a single phase leg of the HV1 AAC. The cell voltages are shown for the top valve in same phase of the HV1 AAC.

TABLE V
TRANSFORMER PARAMETERS IN AAC SYSTEM

Parameter	At 50 Hz	At 350 Hz
Coupling factor	0.995	0.995
Magnetising L	9.7 H	1.4 H
Primary leakage L	48.6 mH	6.9 mH
Secondary leakage L	17.5 mH	2.5 mH

The system's steady-state operation is demonstrated in Figs. 4 and 5. Fig. 4 depicts a selection of system voltages and currents for the system topology utilizing MMCs operated at 350 Hz. Fig. 5 demonstrates the same voltages and currents for a system using AACs at 350 Hz also. Both systems run a 30 MW power flow from the HV1 side to the HV2 side. The cell stacks in the AAC can be seen to generate a much lower peak voltage than those in the MMC as they do not have to support the ac voltage waveform for a full cycle.

In the primary and secondary voltage waveforms shown for the AAC voltage spikes can be noted. These are due to sudden switching of cells to ramp the overlap current to the desired value as quickly as possible due to the brevity of the overlap period.

The ac current is split evenly between both arms whereas the AAC's arms have to conduct the full ac current for a half-cycle each. The ac voltages generated by the AACs are higher than those of the MMCs. This results in lower ac current magnitudes.

As the AAC is operated at the sweet-spot voltage, the energy flows from and to the dc and ac side are well matched. Thus, only moderate balancing currents have to be directed through the arms during the overlap period. The MMC requires a significant dc current to be run through the arms along with half the ac current. Thus, the peak current through the arms is not significantly different in either converter topology. This is important to note as the losses heavily depend on the current magnitudes and the number of devices on the conduction path.

The dc-link currents shown for both systems are measured at the dc output of the converter legs. These currents would still require dc side filtering in a real system which has not been considered in this paper. The dc-link currents from the AACs can be seen to have some high-frequency harmonic content due to the overlap current spikes.

The cell voltages can be seen to be balanced for both system topologies in the bottom graphs in Figs. 4 and 5. The characteristic of the intracycle energy flow shape is indicated through the average cell voltage for both converters at their respective operating points. Furthermore, the two topologies exhibit the same voltage deviation range despite the different number of cells in their stacks. Since the cell capacitors are of the same size in both cases, this indicates that additional space savings can be achieved by using the AAC over the MMC.

III. DESIGN TRADEOFF THROUGH AC-LINK FREQUENCY

The dc/ac/dc system can be optimized for different application areas. For offshore applications, in particular, the volume that the system components require is of particular importance because the entire system has to be housed inside an expensive off-shore platform. The ac frequency has been identified as

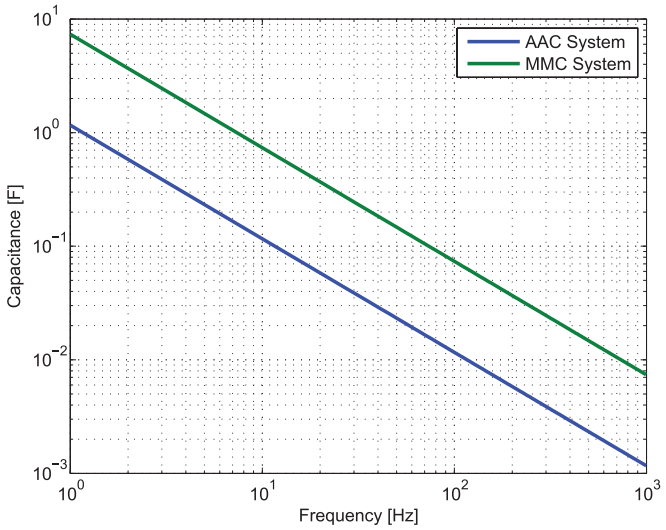

Fig. 6. Minimum capacitance per valve pair for both converter types for case-study dc/ac/dc system across a range of frequencies at unitary power factor operation (10 MW per phase).

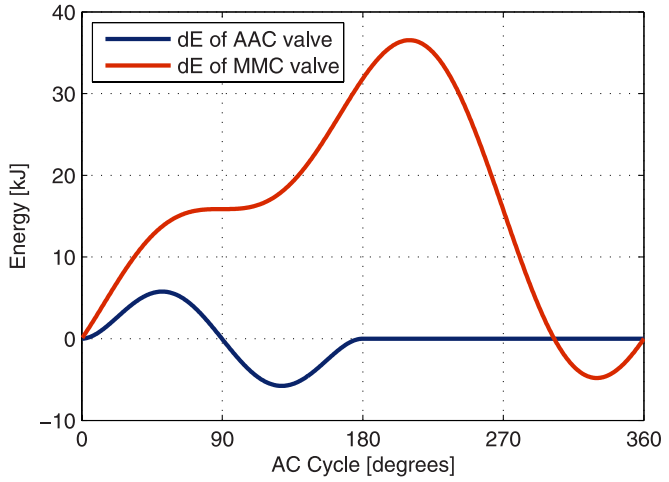

Fig. 7. Energy deviation in top valve of HV1 converter of case study system at 50 Hz and 30 MW power transfer (HV1 to HV2 side) operation.

one parameter which can be used to reduce the system volume: raising the ac frequency reduces the minimum capacitance required in the cells. In theory it also allows for a smaller transformer core.

A. System Volume

To gauge the effect of the frequency on the system volume and compare different topologies against each other, the minimum capacitance per valve pair can be used as per (15). This measure assumes that the voltage band is kept the same for all frequencies and for both converter types

$$\check{C}_{\text{valve pair}} = \check{C}_{c\text{HV1}} \cdot n_{c\text{HV1}} + \check{C}_{c\text{HV2}} \cdot n_{c\text{HV2}}. \qquad (15)$$

Fig. 6 shows the minimum capacitance per valve pair for the case study system for both converter types. A valve pair is considered to be any valve in the HV1 converter and its complimentary valve in the HV2 converter. The diagram clearly shows that a system utilizing MMCs would require a larger capacitance than one using AACs. This is due to the larger intracycle energy deviation experienced by the cell stacks in the MMC as illustrated in Fig. 7.

B. System Losses

Raising the ac frequency requires the cells to switch at a higher frequency also to generate the ac voltage waveform. This causes increased switching losses.

The system losses have been estimated using the time domain data gained from the case-study simulations. Using device-specific loss data, the conduction and switching losses in the semiconductors were calculated by postprocessing the simulation data. Switching occurrences are detected using the gate signals to the cells. Along with these and the current direction and magnitude through the arm a device specific turn-on, turn-off, or diode reverse recovery energy loss is calculated. The switching device assumed in this paper was Toshiba's MG1200FXF1US53. This method assumes that the losses incurred in the devices do not significantly affect the voltage and current waveforms in the system as these power losses are expected to be small.

The transformer losses were estimated using a simplified analytical model. The transformer was taken to consist of a central limb around which first the primary and then the secondary windings are wound. The magnetic path was closed by two outer limbs each with half the cross-sectional area of the central limb. The flux density was chosen according to be 1.72 T and the current density 4 A/mm^2. The model calculates the transformer geometry and associated losses across a range of values of three input variables: the number of secondary turns, the winding height, and the magnetizing current magnitude. This generates several feasible designs and that with minimum power loss was chosen. The same procedure was used for 50 and 350 Hz designs. With the design parameters kept the same, the core volume was reduced by a factor of 7 for the higher frequency case. In the transformer model, cooling requirements have not been taken into consideration. These requirements will typically result in a worse than theoretically possible scaling of the volume of the transformer. Overall the transformer design has not been optimized for 350 Hz operation.

The core losses were calculated based on available data suggested by a manufacturer (which was available for 50 and 350 Hz) and assuming all of the core is at the same flux density. The winding losses were calculated as the simple resistive losses only using the mean turn length and number of turns for each winding. The skin-effect losses were not modeled at this stage because the skin depth of the copper winding at 350 Hz is 3.5 mm which was not significantly smaller than the wire diameter. Tank losses were also not taken into consideration during the modeling of the transformer losses. The loss results are summarized in Tables VI and VII.

TABLE VI
ESTIMATED LOSSES PER PHASE LEG FOR MMC-BASED CASE-STUDY SYSTEM

Loss Type [kW]	At 50 Hz	At 350 Hz
HV1 MMC total	**48.1**	**108.2**
Valve, conduction	36.2	35.7
Valve, switching total	11.4	72.0
Switching due to rotation	*7.3*	*48.1*
Arm inductor, conducting	0.5	0.5
HV2 MMC total	**56.9**	**119.7**
Valve, conduction	39.8	39.0
Valve, switching total	15.8	79.4
Switching due to rotation	*8.7*	*56.4*
Arm inductor, conducting	1.3	1.3
Converters Total	**105.0**	**221.9**
Transformer Total	**47.8**	**47.6**
Winding	41.2	28.9
Core	6.7	18.7
Total	**152.8**	**269.5**
System Efficiency	**98.5%**	**97.4%**

TABLE VII
ESTIMATED LOSSES PER PHASE LEG FOR AAC BASED CASE-STUDY SYSTEM

Loss Type [kW]	At 50 Hz	At 350 Hz
HV1 AAC total	**54.6**	**88.0**
Valve, conduction	32.3	31.4
Valve, switching total	6.6	41.1
Switching due to rotation	*1.7*	*13.2*
DS, conduction	15.5	15.1
Arm inductor, conducting	0.2	0.04
HV2 AAC total	**66.7**	**105.3**
Valve, conduction	39.7	38.2
Valve, switching total	10.2	51.4
Switching due to rotation	*3.1*	*22.0*
DS, conduction	16.2	15.6
Arm inductor, conducting	0.6	0.1
Converters Total	**121.3**	**193.3**
Transformer Total	**46.7**	**47.5**
Winding	40.0	28.8
Core	6.7	18.7
Total	**168.0**	**240.8**
System Efficiency	**98.3%**	**97.6%**

IV. DISCUSSION ON VOLUME AND LOSSES

The losses for the 50 Hz scenario for the MMC are slightly lower than those for the AAC system. This is because the conduction losses in the AAC are slightly higher as the devices that are in the conduction path experience a larger current. The switching losses in the AAC are lower than in the MMC system at 50 Hz as fewer devices are forced to hard switch. This is also the reason why at 350 Hz operation the AAC system suffers lower converter losses than the MMC system. Overall the switching losses increase with increased ac frequency because the switching to generate the ac voltage waveform has to increase proportionally. Furthermore, the cell rotation frequency was kept constant at 16 rotations per cycle so that the capacitor volume could be reduced and so the switching losses due to rotation also increase with frequency. The director switches in the AAC are only opened when the current has been controlled down to zero and therefore suffer no switching losses.

The transformers are winding loss dominated and this term is not greatly different at 50 and 350 Hz. Although the specific core losses are higher at 350 Hz, the volume of core is less. The overall result is that the change in frequency made little difference to the transformer power losses.

The AAC requires smaller total capacitance than the MMC at 50 as well as at 350 Hz. Fig. 6 shows that the AAC can use a capacitance more than six times smaller than the MMC because this application uses the AAC in it most advantageous operating region, namely unitary power-factor at the sweet-spot voltage ratio. Assuming that the cell capacitance takes up about 50 % of the cell volume for a typical MMC application at 50 Hz, an AAC cell would only need to be 58 % of the volume of one for an MMC. Operation at 350 Hz could further reduce the minimum cell volume. While the theoretical minimum capacitance scales inversely with respect to frequency, the added margin for a practical capacitor size may not however scale as well. Similarly, the transformer core theoretically scales inversely with respect to frequency. Due to other design factors associated with the transformer, such as the cooling equipment, the total transformer volume is not expected to scale as well either.

V. CONCLUSION

This paper introduces an HV dc/ac/dc system suitable for interconnecting HVdc networks operated at different dc voltages. The system consists of two front-to-front connected VSCs coupled through a transformer. The ac link is internal to the dc/ac/dc system and therefore the operating frequency can be selected freely and used to tradeoff the volume of the passive components against the power losses in the semiconductor devices.

This study considered modular multilevel converters of either the MMC or AAC format. When operated at 50 or 60 Hz, these converters require cell capacitors which represent approximately 50% of the cell volume. An increase in ac frequency to 350 Hz results in proportionately smaller peak intracycle energy deviations in the cell stacks of both the MMC and AAC. This reduces the minimum capacitance required in both converters and allows a significant reduction in the total system volume. The AAC was found to require a smaller minimum total capacitance than the MMC for all ac frequencies. The use of the AAC at either 50 or 350 Hz frequency would therefore minimize the system volume. The higher frequency also leads to a reduction in transformer volume at a rate a little less than proportional.

The MMC was found to have slightly lower power losses than the AAC at 50 Hz operation. This is due to larger conduction losses in the AAC. At increased ac frequency, however, the switching losses in the MMC were found to increase more quickly than those in the AAC as its operation requires more switching events. The increase in operating frequency changed the balance of core and winding losses in the transformer but did not significantly increase the overall power loss of this component.

Overall, operating the ac link at a frequency of 350 Hz allows for significant volume savings due to the reduced capacitance required in the cell stacks of the converters. This comes at the cost of higher losses in the converters due to increased switching. Using AACs in the system results in lower losses at 350 Hz than using MMCs. Specifically, the losses increased from 504 to 722 kW for a three-phase 30-MW case study system. For an application where converter volume comes at a premium, such as offshore, this increased loss may well be worth accepting for the reduced volume.

ACKNOWLEDGMENT

The authors would like to thank A. Grid for the permission to publish this paper.

REFERENCES

[1] J. Dorn, H. Gambach, and D. Retzmann, "HVDC transmission technology for sustainable power supply," in *Proc. 9th Int. Multi-Conf. Syst., Signals Devices*, Mar. 20–23, 2012, pp. 1–6.

[2] D. Van Hertem, M. Ghandhari, and M. Delimar, "Technical limitations towards a supergrid — A european prospective," in *Proc. IEEE Int. Energy Conf. Exhib.*, Dec. 18–22, 2010, pp. 302–309.

[3] C. D. Barker, C. C. Davidosn, D. R. Trainer, and R. S. Whitehouse, "Requirements of DC–DC converters to facilitate large DC grids," Cigre, SC B4 HVDC and Power Electronics, 2012.

[4] A. Lesnicar and R. Marquardt, "An innovative modular multilevel converter topology suitable for a wide power range," presented at the *IEEE Power Tech Conf.*, Bologna, Italy, 2003.

[5] C. C. Davidson and D. R. Trainer, "Innovative concepts for hybrid multilevel converters for HVDC power transmission," in *Proc. 9th IET Int. AC DC Power Transmiss., Conf.*, Oct. 19–21, 2010, pp. 1–5.

[6] M. M. C. Merlin, T. C. Green, P. D. Mitcheson, D. R. Trainer, R. W. Critchley, and R. W. Crookes, "A new hybrid multi-level voltage source converter with DC fault blocking capability," in *Proc. 9th IET Int. Conf. AC DC Power Transmiss.*, Oct. 19–21, 2010, pp. 1–5.

[7] S. Allebrod, R. Hamerski, and R. Marquadt, "New transformerless, scalable modular multilevel converters for HVDC transmisson," in *Proc. IEEE Power Electron. Special. Conf.*, Rhodes, Greece, Jun. 2008, pp. 174–179.

[8] G. P. Adam, T. C. Lim, S. J. Finney, and B. W. Williams, "Voltage source converter in high voltage applications: Multilevel versus two-level converters," in *Proc. 9th IET Int. Conf. AC DC Power Transmiss.*, 2010, pp. 1–5.

[9] G. T. Son, H.-J. Lee, T. S. Nam, Y.-H. Chung, U.-H. Lee, S.-T. Baek, K. Hur, and J.-W. Park, "Design and control of a modular multilevel HVDC converter with redundant power modules for noninterruptible energy transfer," *IEEE Trans. Power Delivery*, vol. 27, no. 3, pp. 1611–1619, Jul. 2012.

[10] J. A. Ferreira, "The Multilevel Modular DC Converter," *IEEE Trans. Power Electron.*, vol. 28, no. 10, pp. 4460–4465, Oct. 2013.

[11] D. Jovcic, "Bidirectional, high-power DC transformer," *IEEE Trans. Power Delivery*, vol. 24, no. 4, pp. 2276–2283, Oct. 2009.

[12] T. Lüth, M. M. C. Merlin, T. C. Green, C. D. Barker, F. Hassan, R. W. Critchley, R. W. Crookes, D. Trainer, and K. Dyke, "Choice of AC operating voltage in HV DC/AC/DC system," presented at IEEE Power and Energy Society General Meeting *2013*, Vancouver, Canada, Jul. 21–25, 2013.

[13] C. E. Sheridan, M. M. C. Merlin, and T. C. Green, "Assessment of DC/DC converters for use in DC nodes for offshore grids," in *Proc. ACDC. 10th IET Int. Conf. AC DC Power Transmiss.*, 2012, pp. 1–6.

[14] P. Münch, D. Görges, M. Izák, and S. Liu, "Integrated current control, energy control and energy balancing of modular multilevel converters," in *Proc. 36th Annu. Conf. IEEE Ind. Electron. Soc.*, Nov. 2010, pp. 150–155.

[15] S. Rohner, S. Bernet, M. Hiller, and R. Sommer, "Modulation, losses, and semiconductor requirements of modular multilevel converters," *IEEE Trans. Ind. Electron.*, vol. 57, no. 8, pp. 2633–2642, Aug. 2010.

[16] H. Abu-Rub, J. Holtz, J. Rodriguez, and G. Baoming, "Medium-voltage multilevel converters—State of the art, challenges, and requirements in industrial applications," *IEEE Trans. Ind. Electron.*, vol. 57, no. 8, pp. 2581–2596, Aug. 2010.

Thomas Lüth (S'12) received the M.Eng degree (first class Hons.) from Imperial College, London, U.K., in 2010, in electrical and electronic engineering, where he is currently working toward the Ph.D. degree as a member of the Control and Power Research Group under the supervision of Prof. T.C. Green.

His research interests include power electronics and transmission technologies. His work currently focuses on dc/dc converters for HVdc applications.

Michaël M. C. Merlin (M'12) received the Electrical Engineering degree from the Ecole National Supérieur de l'Electronique et de ses Applications (ENSEA), Cergy, France, and the M.Sc. degree in control systems from Imperial College, London, U.K., both in 2008, and the Ph.D. degree in electrical engineering from Imperial College, London, U.K. in 2013.

He is currently working at Imperial College London as a Research Associate. His main research interests include HVdc converter topology, converter control, and HVdc network control.

Tim C. Green (M'89–SM'02) received the B.Sc. (Eng.) degree (first class Hons.) from Imperial College, London, U.K., in 1986, and the Ph.D. degree from Heriot-Watt University, Edinburgh, U.K., in 1990. Both degrees were in electrical engineering.

He is a Professor of electrical power engineering at Imperial College London. His research interest includes in formulating the future form of the electricity network to support low-carbon futures. A particular theme is how the flexibility of power electronics can be used to accommodate new generation patterns and new forms of load as part of the emerging smart grid. He has particular interests in offshore dc networks and of management of low-voltage networks. He leads the HubNet consortium of eight U.K. universities coordinating research in low-carbon energy networks.

Dr. Green is a Chartered Engineer in the U.K.

Fainan Hassan (M'01–SM'13) received the Ph.D. degree in electrical engineering from the Department of Energy and Environment, Chalmers University of Technology, Gothenburg, Sweden, in 2007.

She joined Alstom Grid (then Areva T&D), Research and Technology Centre, Stafford, U.K., in 2009. She has recently been appointed as a Power Electronics Programme Manager at the Research and Technology Centre. Her research interests include the applications of power electronics in the power system, control of power electronics equipment, requirements of power electronics interfacing new resources of electrical energy, distributed generation technologies, control and protection of multiterminal dc grids, and smart grid technologies. She is the coauthor of *Integration of Distributed Generation in the Power system* (Wiley IEEE Press, July 2011).

Carl D. Barker (M'03–SM'09) received the M.Sc. degree in electrical power systems from Bath University, Bath, U.K., in 1989.

He joined Alstom Grid in 1989, initially working on the design and development of individual projects and then managing technical aspects across many projects. He is currently the Chief Engineer, HVdc Grids, within the HVdc Group.

Mr. Barker is a Chartered Engineer and a Member of the IET, CIGRE.